J Solid State Electrochem (1998) 2: 299–307

ORIGINAL PAPER

Aigars Vītiņš · Ģirts Vītiņš · Jānis Krastiņš · Ints Šteins
Ilmārs Zālīte · Andrejs Lūsis

Conductivities and silver electrode polarization resistance of solid electrolyte ceramics from ZrO_2-Y_2O_3 powder synthesized in air plasma

Received: 16 October 1997 / Accepted: 19 January 1998

Abstract Ceramic specimens have been obtained from the powder of ZrO_2-7.5 mol% Y_2O_3 having a specific surface area of 30 m^2/g synthesized in air plasma. The novelty of this research lies in the fact that the plasma process makes it possible to prepare so-called nano-powders with a particle size less than 100 nm, possessing specific physical, chemical and technological properties. The sintered density of the specimens was 94–96% of the theoretical value, 6.001 g/cm^3. The X-ray diffraction pattern of the specimens corresponded to a face-centered cubic lattice. Impedance in the frequency range of 100 Hz–15 MHz and d.c. polarization curves in a potential range of −10 to 10 mV were measured in the temperature range 200–850 °C in heating and cooling cycles. The intragrain, the grain boundary and the total bulk conductivities, the electrode polarization resistance and their activation energies were determined. The thermal stability of the studied system was proved in three measurement series up to 600–850 °C in heating and cooling cycles. The results obtained have shown that the conductivity of ZrO_2-7.5 mol% Y_2O_3 ceramics is not solely a function of temperature, but also depends on the previous thermal state of the ceramics.

Key words Yttria-stabilized zirconia · Plasma synthesis · Ceramics · Impedance · Ion conductivity

A. Vītiņš (✉) · Ģ. Vītiņš · A. Lūsis
Institute of Solid State Physics, University of Latvia,
Ķengaraga ielā 8, LV-1063 Riga, Latvia
Tel.: +371-7187817; Fax: +371-7112583;
e-mail: vitinsa@com.latnet.lv

J. Krastiņš · I. Šteins · I. Zālīte
Institute of Inorganic Chemistry,
the Latvian Academy of Sciences, Miera ielā 34,
LV-2169 Salaspils, Latvia

Introduction

Yttria-stabilized zirconia (YSZ) is widely known as a high-temperature solid electrolyte with oxygen ion conductivity [1–3]. A possible application of YSZ in a solid oxide fuel cell determines the interest in YSZ materials [1–4].

The plasma technique enables high-melting compounds, such as YSZ, to be obtained as a very fine powder with a particle size of less than 100 nm, possessing specific physical, chemical and technological properties [5–7]. The desired amount of yttria can be added to zirconia during plasma synthesis of YSZ. One of the objects of this research was to study the sintering properties of plasma powders of YSZ.

Impedance spectroscopy for solid electrolyte conductivity studies was proposed for the first time in [8]. Since then, the impedance technique has been used in many conductivity studies of YSZ, for instance [4, 9–13]. The significance of the impedance technique is that it enables one to separate the contributions of the intragrain and grain boundary resistances from the polarization resistance of electrode processes in the total d.c. resistance of a ceramic specimen with reversible electrodes [4, 8–11, 13]. The interest of conductivity studies for ceramics from ZrO_2-7.5 mol% Y_2O_3 synthesized in plasma is a consequence of the fact that the starting material, small impurities, the preparation technique, the thermal treatment and the cooling procedure have a considerable effect on the conductivity of ceramics [4, 8, 9]. The application of impedance and d.c. polarization had the following objectives in our research: to study the conductivity of the YSZ ceramics, i.e. to determine the contributions of intragrain and grain boundary resistances in the temperature range 200–850 °C, to check the thermal stability of the conductivity in the measurement series in heating and cooling cycles, and to determine the polarization resistivity of electrode processes for the cell of Ag/YSZ/Ag in air in the temperature range 400–814 °C.

Experimental

ZrO_2-7.5 mol% Y_2O_3 powder

ZrO_2-7.5 mol% (13.0 wt%) Y_2O_3 powder was synthesized in air plasma from a mixture of zirconia and yttria under conditions similar to those described in [5, 7]. The powder had a specific surface area of 30 m^2/g, which corresponds to a mean size of the particles of 33 nm, assuming a spherical shape of the particles [5–7]. The Y_2O_3 content (13.0 wt%) in the synthesized ZrO_2-Y_2O_3 powder was determined by chemical analysis.

Preparation of ceramics

The ZrO_2-7.5 mol% Y_2O_3 powder was plasticized by adding solution of 2 wt% oleic acid in acetone and milling in a ball mill for 24 h. The plasticized powder was dried at 100–120 °C and sieved (sieve opening 0.016 mm). Disk-shaped specimens were prepared by uniaxially cold pressing the sieved powder to 81–323 MPa in a cylindrical hardened steel die. The plasticizer was burned out of the green compacts at 600–650 °C. The specimens were sintered at 1530 °C in a nitrogen gas atmosphere for 4 h in a molybdenum resistance vacuum furnace CWB-1.2,5/25 n1 (U.S.S.R.). The heating rate was 600 °C/h.

For conductivity studies it is essential to remove the glassy phase from the surface of the ceramic specimen. For this purpose, wetted flat surfaces of ceramic specimens were ground on a rotating diamond ring. The conductivity of one ground specimen was studied.

Density of ceramics

The density of a ceramic specimen was measured from specimen dimensions and weight and by means of the Archimedes method using distilled water as the medium. A ceramic specimen was plunged in distilled water and brought under vacuum to fill its pores with water. The pycnometric volume of the specimen was determined by the Archimedes method. The volume of open pores of the specimen was determined from the difference between the weights of the wet and dry specimens. The apparent volume of the specimen was defined as a sum of the pycnometric volume and the volume of open pores. The apparent density was defined as the ratio of the mass of the dry specimen to its apparent volume. The geometric volume was determined from specimen dimensions. The geometric density was defined as the ratio of the mass of the dry specimen to its geometric volume. The theoretical density was assumed to be 6.001 g/cm^3, as proposed in [4] for ZrO_2-8 mol% Y_2O_3.

Open porosity and densities for the specimen used in conductivity studies are given in Table 1. The specimen had no measurable open porosity. The values of the open porosity (≤0.2 vol%) and the pycnometric density (96.3% of the theoretical value 6.001 g/cm^3) can be explained as the pores are local and do not connect throughout the ceramics. The fact that the value of the geometric density is lower than that of the apparent density may be due to irregularities in specimen shape.

Ceramic microstructure

The ceramic microstructure was revealed by thermal etching of the polished specimen at 1400 °C for 1 h [11]. Scanning electron micrographs of magnifications 1900 and 6200 times showed grain boundaries and grains. Not all grain boundaries were distinct on the micrographs, so that the average grain size can be only estimated to be approximately ≤10 μm. The micrographs also showed pores. Micropores up to ca. 1–3 μm in size were located mainly at grain boundaries and triple points of grain boundaries, but some micropores also appeared to be located within grains. Micrographs also showed pores up to 5–10 μm in size to be present in ceramics. Small shallow pits of ca. ≤1 μm in size were seen on the grain surface in a micrograph of magnification 6200 times. The shallow pits can be attributed to exits of dislocations on the grain surface.

X-ray diffraction study

The phase composition of an as-sintered specimen and a ceramic specimen ground into powder was studied by X-ray diffraction (XRD) using Cu Kα radiation ($\lambda = 1.54184$ Å). The XRD patterns corresponded to a face-centered cubic lattice with the length of the side of the unit cell $a = 5.138 \pm 0.003$ Å. The value of the lattice parameter for our ZrO_2–7.5 mol% Y_2O_3 (i.e. $Y_{0.14}Zr_{0.86}O_{1.93}$) is in agreement with the literature data for $Y_{0.15}Zr_{0.85}O_{1.93}$, $a = 5.139(1)$ Å [14].

Electrodes

The specimen whose electrophysical properties were studied had a cross-section surface $S = 0.827$ cm^2, thickness $H = 0.183$ cm, and the cell constant $H/S = 0.221$ cm^{-1}. The conductivity of the ceramic specimen was investigated by a two-electrode technique. Silver electrodes were applied to both ground flat faces of the disk-shaped specimen. These electrodes were formed on the specimen by the decomposition of a 57 wt% Ag_2CO_3 paste with colophony and turpentine. The paste coating on a specimen face was dried at 140–152 °C for 15 min. Then the specimen, with both faces coated, was heated in air to 850 °C for 2 h, held for 2 h at 850 °C, and cooled as the furnace cooled. Observations in an optical microscope (magnification 10–60 times) revealed the silver electrodes to be rather porous. The average mass per unit area of the silver electrodes was 6.7 mg/cm^2. The sheet resistance of the electrode layer was measured between two points on it, and was 0.01–0.03 Ω.

Impedance measurements

Impedance measurements were made with an HP 4194A impedance analyzer (Hewlett-Packard) over the frequency range 100 Hz–15 MHz at the oscillation level ≤10 mV rms with a long integration time and the weighting factor (NOA – number of averaging) equal to 1 unless otherwise stated. A high oscillation level, up to 500 mV, was used in dielectric measurements at room temperature (12–25 °C) and high impedance (more than 100 kΩ) measurements at 200–275 °C.

A high-temperature specimen holder with two silver leads was used to make impedance measurements of the specimen. An HP 16334A test fixture (a cable length of ca. 1 m) was used to interconnect leads of the holder and terminals of the HP 4194A impedance analyzer.

Impedance short measurements for the specimen holder were made at room temperature and over the range of 500–850 °C to compensate the impedance of lead wires of length ca. 0.44 m each

Table 1 Open porosity and densities of the ceramic specimen

Open porosity (vol %)	Pycnometric density (g/cm^3)	(% theoret.)	Apparent density (g/cm^3)	(% theoret.)	Geometric density (g/cm^3)	(% theoret.)
≤0.2	5.777	96.3	5.771	96.2	5.681	94.7

from measured impedance spectra of the specimen in the holder. At room temperature, lead wires had resistance ca. 0.25 Ω and inductance ca. 0.8 μH. At 850 °C, lead wires had resistance ca. 0.4 Ω and inductance ca. 0.8 μH. The residual capacitance of the specimen holder was found to be ca. 0.5 pF.

Impedance spectra were measured at a constant temperature. The constancy of temperature was maintained within ±1 °C. To obtain the temperature dependence of the conductivity, the series of impedance measurements at different constant temperatures were made. A sequence of measurements as the temperature was raised is called a heating cycle. A sequence of measurements as the temperature was decreased is called a cooling cycle. Impedance measurements were made over the temperature range 200–850 °C, normally at 25–40 °C temperature intervals during heating and cooling cycles. Three impedance measurement series were made: (1) from 276 to 602 °C during a heating cycle (duration ca. 5 h 15 min) and back from 602 to 350 °C during a cooling cycle (duration ca. 5 h 20 min), (2) from 200 to 850 °C during a heating cycle (duration ca. 5 h 20 min) and back from 850 to 300 °C during a cooling cycle (duration ca. 7 h 40 min), and (3) from 200 to 405 °C during a heating cycle (duration ca. 3 h 50 min). Then the temperature was stabilized in the vicinity of 400 °C, and both impedance and potentiostatic polarization measurements were made. The technique of potentiostatic polarization measurements is described in the following section. Both impedance and potentiostatic polarization measurements were made at selected constant temperatures from 398 to 814 °C during a heating cycle (duration 11 days) and back from 814 to 606 °C during a cooling cycle (duration 6 days), and final impedance measurements were made at 600 and 575 °C in this series.

After each measurement series the specimen, in the furnace, was cooled down to room temperature as the furnace cooled.

Direct current polarization measurements

Polarization measurements under a constant voltage from −10 to 10 mV were made to study direct current (d.c.) properties of the two-electrode cell, Ag/YSZ/Ag, in air. A potentiostat PAR 173 (Princeton Applied Research, Princeton, N.J.) was used. The cell voltages were measured by means of an additional voltmeter B7-46 (Belvar, Minsk, Belorussia) external to the PAR 173 potentiostat. Stabilization of the cell current was observed on a chart recorder RE 511 (Servogor). The cell current stabilized within less than 2 min at a constant value of the cell voltage and at a temperature of 562–814 °C. The stabilized values of the cell current were plotted against the values of the cell voltage to obtain the current-voltage characteristics of the cell. Direct-current polarization measurements of two-electrode cells with solid-oxide electrolyte are described in [15].

Results and interpretation

Impedance complex-plane plots

Complex-plane impedance data plots are useful in identifying the physicochemical processes involved in the electrical response of the specimen [16]. Impedance complex plane plots for 425 °C are shown in Fig. 1. Macroscopic specific impedance is plotted taking into account the cell constant $H/S = 0.221\ \mathrm{cm}^{-1}$. Impedance plots contain two arcs.

Impedance complex-plane plots were interpreted according to a simplified equivalent circuit proposed in the literature [8–10, 13, 16]:

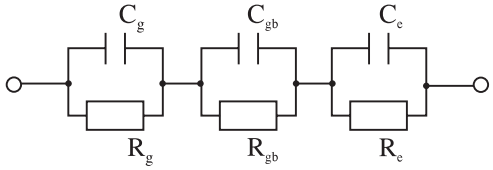

where C_g is the geometrical capacitance, C_{gb} the grain boundary capacitance, C_e the electrode capacitance, R_g the intragrain resistance, R_{gb} the grain boundary resistance, and R_e the electrode polarization resistance. In the case when $R_gC_g \ll R_{gb}C_{gb} \ll R_eC_e$, the contributions of R_g, R_{gb} and R_e can be derived from impedance plots to a high accuracy by simple geometrical methods [9, 10, 13]. The high-frequency arc on the left in Fig. 1 is due to the intragrain resistivity, and the arc on the right (next to the intragrain resistivity arc) is due to the grain boundary resistivity [4, 9, 10, 13]. The real specific impedance sections between the distinct minima in the capacitive reactance, -Im(Z), correspond to the macroscopic specific resistivities of the grains $R_g \times S/H$ and the grain boundaries $R_{gb} \times S/H$, respectively. The total bulk resistance R_t is defined as $R_t = R_g + R_{gb}$. The intragrain conductivity σ_g, the grain boundary conductivity σ_{gb} and the total bulk conductivity σ_t are defined by the following equations: $\sigma_g = (H/S) \times (1/R_g)$, $\sigma_{gb} = (H/S) \times (1/R_{gb})$ and $\sigma_t = (H/S) \times (1/R_t)$.

Impedance plots measured in two measurement series in both heating and cooling cycles enable us to appreciate the reproducibility of the conductivity properties of the specimen of Ag/ZrO_2–7.5 mol% Y_2O_3/Ag and to appreciate the effect of the previous thermal state of the specimen on its conductivity. In the first measurement series up to 602 °C impedance curves at 425 °C for the heating and the cooling cycles are close (curves 1 and 2 of Fig. 1). In the second series up to 850 °C there is an appreciable difference between impedance curves at 425 °C for the heating and the cooling cycles (curves 3 and 4 of Fig. 1) meaning a decrease by ∼14% and ∼27% for intragrain and grain boundary conductivities, respectively. The observed trend for the conductivity of our YSZ at 425 °C is that in a cooling cycle the con-

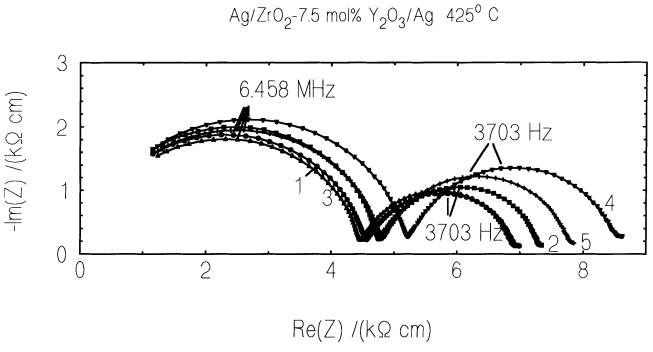

Fig. 1 Impedance plots (100 Hz–15 MHz) measured in heating (*1, 3, 5*) and cooling (*2, 4*) cycles of the first (*1, 2*), the second (*3, 4*) and the third (*5*) measurement series for the specimen of Ag/ZrO_2-7.5 mol% Y_2O_3/Ag at 425 °C in air. NOA = 1

ductivity is lower than that in a heating cycle in the same series (compare curves 2 vs 1 and 4 vs 3 of Fig. 1). Cooling down to room temperature restores the conductivity of our YSZ at 425 °C completely or in part (compare curves 3 vs 2 and 5 vs 4 of Fig. 1).

Direct current properties of the system of Ag/ZrO_2-7.5 mol% Y_2O_3/Ag in air

Current-voltage characteristics obtained from potentiostatic polarization measurements of the system at 606 °C are shown in Fig. 2. The current-voltage characteristics were linear in the studied temperature range of 400–814 °C. From reciprocal values of their slopes, the values of the direct current (d.c.) resistance R_{dc} were determined. The values of R_{dc} were corrected for the resistance of the silver leads. According to the equivalent circuit described in the previous section, the d.c. resistance is given by $R_{dc} = R_g + R_{gb} + R_e = R_t + R_e$. The electrode polarization resistance R_e can be calculated as the difference between the total bulk resistance R_t determined from an impedance plot and the d.c. resistance R_{dc}. Impedance plots together with R_{dc} values on real axes are shown in Fig. 3. At 606 °C only a small part have remained from the intragrain arc, and only the grain boundary arc is complete (Fig. 3a). The part of the arc on the extreme right (appearing on the low-frequency end of the impedance plot) is due to the relaxation of the electrode processes [4, 9, 10]. At 606 °C the impedance plots have two distinct minima, and thus R_g, R_{gb} and R_e can easily be determined from the data in Fig. 3a.

The grain boundary arc and part of the electrode arc are present in the plot at 752 °C (Fig. 3b). Low-frequency data points of the electrode arc are scattered. The use of the high weighting factor (NOA), up to 256,

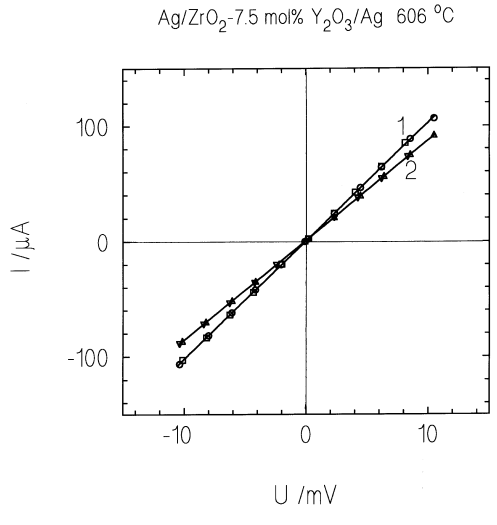

Fig. 2 Current-voltage characteristics for the specimen of Ag/ZrO_2-7.5 mol% Y_2O_3/Ag at 606 °C in air measured in the heating (*1*) and the cooling (*2*) cycles. Successive values of the voltage were increasing (O, Δ) and decreasing (□, ∇)

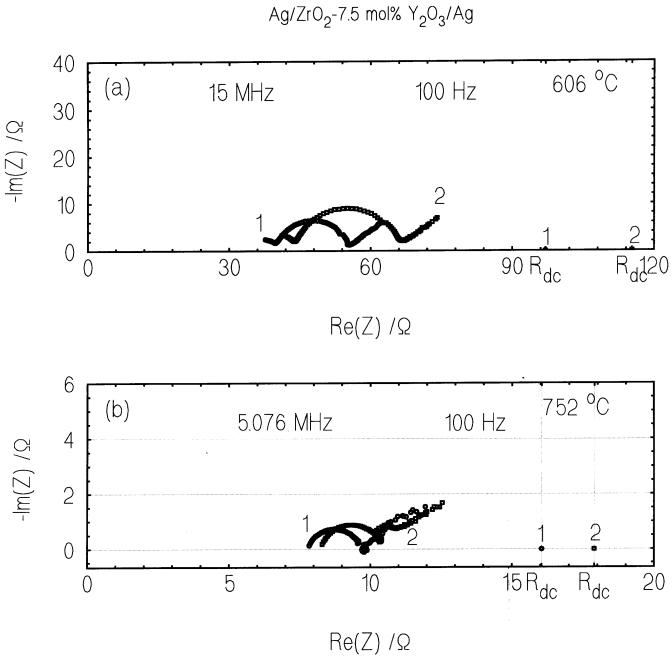

Fig. 3a, b Impedance plots in the frequency ranges of 100 Hz–15 MHz (**a**) and 100 Hz–5.076 MHz (**b**) and values of the d.c. resistance R_{dc} on the real axis for the specimen of Ag/ZrO_2-7.5 mol% Y_2O_3/Ag at 606 °C (**a**) and 752°C (**b**) in air measured in the heating (*1*) and the cooling (*2*) cycles of the third measurement series. Impedance plots were measured at a weighting factor (NOA) for **a** and *1***b** of 1, and for *2***b** of 256

can reduce scatter in the impedance data points and thus give a smooth impedance curve. However, short measurements only at NOA = 1 have been made. Curve 2 of Fig. 3b is the impedance curve measured at NOA = 256 and compensated by the short measurement at NOA = 1. Such compensation significantly distorts the impedance curve 2 of Fig. 3b in the vicinity of the second minimum of the capacitive reactance -Im(Z). However, the values of R_t and R_e can be estimated from the data in Fig. 3b.

To characterize the polarization properties of the electrodes, the polarization resistivity r_e was calculated $r_e = R_e \times S/2$.

Temperature dependences of conductivities

Ionic conductivity of a solid electrolyte is thermally activated process. According to the theory of ionic transport in a solid electrolyte [17], the ionic conductivity σ depends on the absolute temperature T according to the equation

$$\sigma = \frac{\sigma_0}{T} e^{-E_a/kT},$$

where E_a is the activation energy, σ_0 a constant, k the Boltzmann constant (8.617×10^{-5} eV/K). Thus a meaningful representation of the temperature dependence of conductivity is a plot of lg(σT) against $1/T$. The Arrhenius plot should be a line with slope a, such that the activation energy $E_a = -2.303 \times k \times a$.

The $\log_{10}(\sigma T)$ against $1/T$-plots of conductivities of YSZ in the temperature range 200–850 °C are given in Fig. 4. The activation energy values in three measurement series both in heating (h) and cooling (c) cycles for conductivities σ_g, σ_{gb} and σ_t in different temperature ranges ΔT are summarized in Table 2. The deviation in the last digit of an activation energy value in the 95% reliability interval is given in brackets after the activation energy value.

The decrease in the slope of $\lg(\sigma_g T)$ against $1/T$-curves at 425–500 °C corresponds to a decrease in the activation energy of the intragrain conductivity from 1.09–1.11 eV to 1.00–1.05 eV. Above 600 °C the activation energy of the intragrain conductivity further decreased to 0.95–0.99 eV. The character of the change in the intragrain activation energy is observed both in heating and cooling cycles of three measurement series (Table 2).

The conductivity of the grain boundaries has the activation energy 1.14–1.20 eV, which is higher by ca. 0.1 eV than that for the intragrain conductivity and is comparatively independent of temperature.

The total bulk conductivity according to its definition (see the Section "Impedance complex-plane plots") is a function of both the intragrain and the grain boundary conductivities. The activation energy of the total bulk conductivity decreases from 1.12–1.17 eV to 0.94–0.98 eV in the studied temperature range from 350 to 850 °C (Table 2). At temperatures above 600 °C the activation energy values of the total bulk conductivities become similar to those of the intragrain conductivities.

Temperature dependence of the electrode polarization resistivity

Temperature dependence of the electrode polarization resistivity r_e can be described by an empirical Arrhenius equation [2, 8, 15]:

$$\frac{1}{r_e} = \frac{1}{r_0} e^{-E_a/kT},$$

where E_a is the activation energy, r_0 a constant, and k the Boltzmann constant. Thus, to obtain a line the values of $\log(1/r_e)$ should be plotted against $1/T$. The activation energy can be obtained from the slope of the line.

The Arrhenius plots of polarization resistivity are shown in Fig. 5. The activation energy of the electrode polarization resistivity r_e for the system Ag/ZrO_2-7.5 mol% Y_2O_3/Ag in air was found to be 0.95 ± 0.06 eV in the range 562–814 °C of the heating cycle and 1.05 ± 0.02 eV in the range 606–814 °C of the cooling cycle. The deviation of the activation energy value is given in the 95% reliability interval.

Discussion

The conductivity of ceramics

Comparison of conductivity values with literature data

As yttria-stabilized zirconia is a widely known solid electrolyte [1–3] and its conductivity is studied in nu-

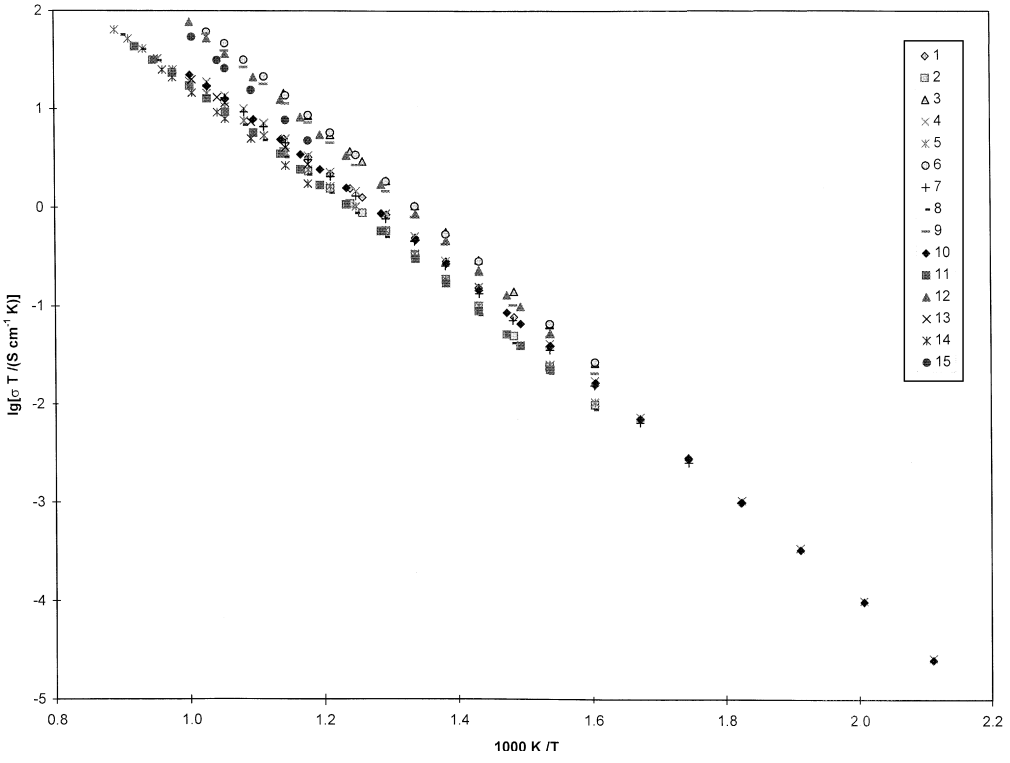

Fig. 4 $\log_{10}(\sigma T)$ against $1/T$ plots of the intragrain (*1, 4, 7, 10, 13*), the grain boundary (*3, 6, 9, 12, 15*) and the total bulk (*2, 5, 8, 11, 14*) conductivities of the ZrO_2-7.5 mol% Y_2O_3 specimen measured in heating (*1–6, 10–12*) and cooling (*7–9, 13–15*) cycles of the first (*1–3*), the second (*4–9*) and the third (*10–15*) measurement series

Table 2 Activation energy values for conductivities of ZrO_2-7.5 mol% Y_2O_3

σ	Series	Cycle						
g	1	h	ΔT,°C	276–425	425–500	500–602		
			E_a, eV	1.11 (1)	1.06 (2)	1.011 (4)		
g	1	c	ΔT,°C	350–425	425–500	500–602		
			E_a, eV	1.11 (2)	1.068 (2)	1.031 (2)		
g	2	h	ΔT,°C	200–425	425–528	528–600	600–700	
			E_a, eV	1.103 (3)	1.054 (6)	1.012 (7)	0.96 (2)	
g	2	c	ΔT,°C	300–475		475–575	575–700	
			E_a, eV	1.095 (4)		1.045 (7)	0.99 (1)	
g	3	h	ΔT,°C	200–475		475–640	640–700	
			E_a, eV	1.095 (3)		1.006 (4)	0.95 (4)	
g	3	c	ΔT,°C			575–641	675–722	
			E_a, eV			1.009 (6)	0.96 (3)	
gb	1	h	ΔT,°C		425–552	552–602		
			E_a, eV		1.143 (5)	1.20 (7)		
gb	1	c	ΔT,°C		350–602			
			E_a, eV		1.179 (4)			
gb	2	h	ΔT,°C		450–552	552–675		
			E_a, eV		1.19 (1)	1.15 (1)		
gb	2	c	ΔT,°C		425–575	575–675		
			E_a, eV		1.203 (4)	1.17 (2)		
gb	3	h	ΔT,°C	377–475		475–700		
			E_a, eV	1.196 (7)		1.143 (5)		
gb	3	c	ΔT,°C			575–686		
			E_a, eV			1.18 (2)		
t	1	h	ΔT,°C	350–425	425–500	500–602		
			E_a, eV	1.17 (1)	1.09 (2)	1.054 (6)		
t	1	c	ΔT,°C	350–475		475–602		
			E_a, eV	1.124 (9)		1.078 (4)		
t	2	h	ΔT,°C	350–425	425–528	528–625	625–725	725–850
			E_a, eV	1.14 (2)	1.09 (1)	1.048 (9)	0.98 (1)	0.94 (1)
t	2	c	ΔT,°C	350–475		475–575	575–725	725–850
			E_a, eV	1.127 (4)		1.099 (6)	1.037 (7)	0.982 (5)
t	3	h	ΔT,°C	377–475		475–640	640–752	
			E_a, eV	1.120 (5)		1.050 (4)	0.994 (3)	
t	3	c	ΔT,°C				575–812	
			E_a, eV				1.055 (7)	

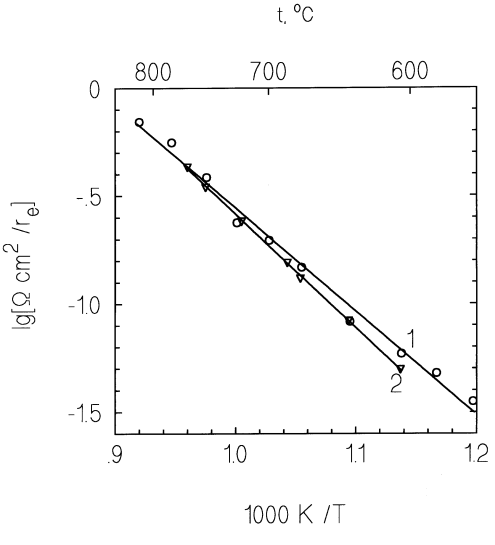

Fig. 5 Arrhenius plots of the electrode polarization resistivity r_e for the system Ag/ZrO_2-7.5 mol% Y_2O_3/Ag in air for the heating (*1*) and cooling (*2*) cycles

merous papers, e.g. [2, 4, 8–13], an important point of our study is the comparison of the conductivity of ceramics from ZrO_2-7.5 mol% Y_2O_3 synthesized in plasma with the conductivity values for ceramics of ZrO_2–ca. 8 mol% Y_2O_3 reported in the literature [4, 9, 11].

The values of the intragrain and the total bulk conductivities of our ZrO_2-7.5 mol% Y_2O_3 ceramics at selected temperatures in the heating cycle of the third measurement series are compared with the relevant literature data in Table 3. The YSZ ceramics of the literature [4, 9, 11, 12] given in Table 3 were sintered at 1500 °C in air for 3 [9], 4 [4] and 5 [12] h. The comparison given in Table 3 shows the agreement of the conductivity values of our ZrO_2-7.5 mol% Y_2O_3 ceramics with the literature data.

As pointed out in [4, 9], the resistivity of grain boundaries is very sensitive to the content of impurities in the specimen. We have not analyzed our specimens for impurity content. The intragrain and grain boundary resistivities of our specimen at 350 °C (37–41 and 24–31 k$\Omega \times$ cm, respectively) are in line with the literature data [4] for ZrO_2-7.6–8.9 mol% Y_2O_3 specimens. This means that the impurity content of our specimen had no significantly larger effect on the resistivity values than did the impurity contents of specimens made from

Table 3 Comparison of the intragrain (σ_g) and the total bulk (σ_t) conductivities of our ZrO_2-7.5 mol% Y_2O_3 with the literature data

	Temperature (°C)	Conductivity (mS/cm) Our ZrO_2-7.5 mol% Y_2O_3	YSZ studied in the literature	Y_2O_3 content (mol%) of the literature YSZ	Density of the literature YSZ (% theoret.)	Remarks on the literature YSZ	The literature source
σ_g	290	0.0032	0.0033	6.15, 8.27	95 ± 2	ultrafine coprecipitated powders	[11]
	450	0.373	0.412	7.5	96.1	commercial Zircar powder	[9]
	450	0.373	0.5	7	–	Tosoh powder	[12]
	500	1.03	1	8.27	95 ± 2	ultraf. coprecipit. p.	[11]
σ_t	600	3.6	5.6	7.78	99.3	Tosoh powder	[4]
	800	34	55	7.78	99.3	Tosoh powder	[4]

commercial powders of ZrO_2- ca. 8 mol% Y_2O_3 nominal composition studied in [4].

Effect of thermal treatment on the conductivity

Three series of impedance measurements in both heating and cooling cycles have shown that the conductivity is not solely a function of the temperature, but also depends on the previous thermal state of the specimen. This means a difference between the conductivities in heating and cooling cycles and a difference between the conductivities in different measurement series (see for instance Figs. 1 and 4).

In the first measurement series up to 602 °C the difference in the conductivities in the heating and cooling cycles is small (Figs. 1 and 4), but in the second and the third measurement series up to 814–850 °C an appreciable difference in both the intragrain and in the grain boundary conductivities has been observed for heating and cooling cycles (Figs. 1 and 4). The difference in the case of the grain boundary conductivity σ_{gb} is greater than that in the case of the intragrain conductivity σ_g. The effect of thermal treatment on the intragrain and the grain boundary conductivities of ZrO_2- ca. 8 mol% Y_2O_3 ceramics is studied and discussed in some respects in [4].

To compare conductivities in different measurement series, the conductivities are plotted in the following units: the σ_g, σ_{gb} and σ_t values at 425 °C of the heating cycle of the first series are taken as 100, i.e., for σ_g 100 units are equal to 0.219 mS/cm, for σ_{gb} 100 units are 0.418 mS/cm and for σ_t 100 units are 0.144 mS/cm (see Fig. 6). Apart from the already dicussed trend that the conductivities during the cooling cycle are lower than those for the heating cycle, an interesting feature of restoration of conductivities is observed (Figs. 1 and 6), i.e. the conductivities in the h-2 cycle are greater than those in the c-1 cycle and the conductivities in the h-3 cycle are greater than those in the c-2 cycle. This means that some changes occur in the ceramics of ZrO_2-7.5 mol% Y_2O_3 at temperatures below 425 °C, leading to the observed restoration of conductivity.

Taking into account the high activation energies of conductivities, i.e. the strong dependence of conductivities on temperature, the discussed effects are small. The observed differences in conductivities can be compensated by a small temperature change. For instance, in the second measurement series, a temperature increase from 425 °C to 431.2 °C can compensate the decreased value of the intragrain conductivity $\sigma_g = 0.192$ mS/cm at 425 °C in the cooling cycle in comparison with the σ_g value of 0.224 mS/cm in the heating cycle at 425 °C. This means that the conductivity values are reproducible in different measurement series both in heating and cooling cycles. Thus we can conclude that the investigated ceramic specimen of ZrO_2-7.5 mol% Y_2O_3 is thermally stable.

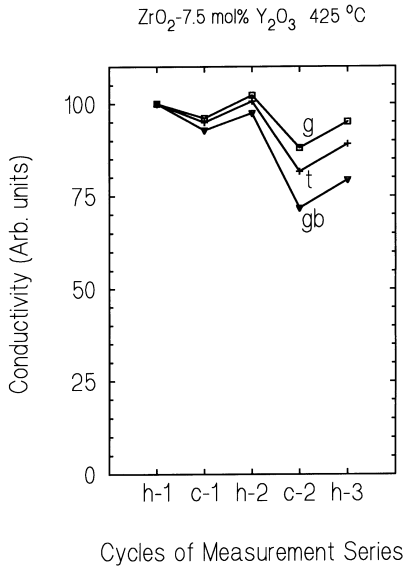

Fig. 6 Comparison of the values of the intragrain (g), the grain boundary (gb) and the total bulk (t) conductivities of the specimen of Ag/ZrO_2-7.5 mol% Y_2O_3/Ag at 425 °C in air measured in heating (h) and cooling (c) cycles of three measurement series (*1–3*). The values of the conductivities are expressed in arbitrary units (see text)

Activation energies of the conductivities

The activation energy values for the conductivities of our specimen (Table 2) are in general agreement with the

literature data [4, 9]. The characteristic feature of the activation energy of the intragrain conductivity of our ZrO_2-7.5 mol% Y_2O_3 is its decrease from 1.10 eV to 0.95–0.99 eV with increase of temperature from 200 to 700 °C (Table 2). A similar decrease in the activation energy of the intragrain conductivity was observed in the literature [4, 9]. The grain boundary activation energy showed no significant changes with the temperature. No bend in the Arrhenius plots of the grain boundary conductivities was observed in [9].

The decrease in the activation energy of the total conductivity from 1.12–1.17 eV to 0.94–0.98 eV in the temperature range from 350 to 850 °C (Table 2) can be explained, as the total bulk conductivity has contributions from both grains and grain boundaries. Because of the higher activation energy of grain boundaries, their contribution to the total conductivity considerably decrases at temperatures above 600 °C, and thus at high temperatures the total bulk conductivity and its activation energy are determined mainly by the intragrain conductivity and its activation energy, respectively. This phenomenon was discussed in [4, 11, 13].

The polarization resistivity of electrode processes in the system of Ag/ZrO_2-7.5 mol% Y_2O_3/Ag in air

The obtained values of the polarization resistivity are macroscopic characteristics of the studied system. Polarization resistivity in the cooling cycle was ca. 26% greater than that in the heating cycle of the third series at 606 °C. This indicates fair electrode stability in the studied temperature range 606–814 °C. Our values of the polarization resistivity are lower by a factor of 2–4 than those for Ag/ZrO_2-8 mol% Y_2O_3/Ag in air obtained in [18]. This indicates a somewhat better performance of our electrodes in comparison with those studied in [18]. The activation energy of the polarization resistance is in agreement with the literature data [18].

Conclusions

1. Qualitative ceramic specimens have been obtained from ZrO_2-7.5 mol% Y_2O_3 powder synthesized in air plasma (the specific surface area of the powder was 30 m^2/g). Sintered density of the specimens was 94–96% of the theoretical value, 6.001 g/cm^3. The X-ray diffraction pattern of the specimens corresponded to the face-centered cubic lattice with the length of the side of the unit cell $a = 5.138 \pm 0.003$ Å.
2. Direct current polarization curves were measured in a potential range of −10 to 10 mV and in the temperature range of 400–814 °C. The d.c. polarization curves were linear. From the impedance data and slopes of the d.c. polarization curves, the polarization resistance of electrode processes in the system Ag/ZrO_2-7.5 mol% Y_2O_3/Ag in air was calculated to be 1.7 $\Omega \times cm^2$ at 800 °C and 18–23 $\Omega \times cm^2$ at 600 °C. The activation energy of the polarization resistance was found to be 0.95 ± 0.06 eV in the range 562–814 °C of the heating cycle and 1.05 ± 0.02 eV in the range 606–814 °C of the cooling cycle. Direct-current polarization and impedance curves demonstrated fair thermal stability of the studied system, Ag/ZrO_2-7.5 mol% Y_2O_3/Ag, in air at temperatures up to 814 °C.
3. Impedance plane plots (100 Hz–15 MHz) had two distinct arcs at 350–425 °C. The arcs were attributed to the intragrain and the grain boundary resistivities: 37–41 and 24–31 $k\Omega \times cm$ at 350 °C, respectively. This is in agreement with the literature data [4] for ceramic specimens made from commercial powders of ZrO_2-(7.6–8.9) mol% Y_2O_3. Because of the particularly strong effects of several impurities such as SiO_2 and Al_2O_3 on the grain boundary resistivity in the low-temperature range (e.g. at 350 °C) [4], we can conclude that the level of such impurities in our specimen is comparable with that for specimens made from commercial powders.
4. The ceramic specimen of ZrO_2-7.5 mol% Y_2O_3 showed good thermal stability in three successive measurement series both in heating and cooling cycles up to 600–850 °C. In a cooling cycle, both the intragrain and the grain boundary conductivities were lower than those for a corresponding heating cycle by up to 15% and 30%, respectively. Some restoration of the conductivities at 425 °C was observed after cooling down from 425 °C to room temperature (12–25 °C). Results obtained have shown that conductivity of ZrO_2-7.5 mol% Y_2O_3 ceramics is not solely a function of temperature, but also depends on the previous thermal state of the specimen.
5. The activation energy of the intragrain conductivity decreased from 1.10 eV to 0.95–0.99 eV in the temperature range from 200 to 700 °C, and that for the grain boundary conductivity was 1.14–1.20 eV, with no significant temperature dependence in that temperature range. The values and behavior of the activation energies are in agreement with the literature data [4, 9].
6. The total bulk conductivity was estimated to be 38–33 mS/cm at 800°C and is comparable with the literature data [4].
7. Plasma synthesis can produce yttria-stabilized zirconia powder suitable for fabrication of ceramics appropriate for solid oxide fuel cell application.

Acknowledgements This work was financially supported by grants Nos. 93.664 and 96.676 from the Latvian Council of Science. The authors would like to thank Dr. Jānis Grabis (Institute of Inorganic Chemistry, the Latvian Academy of Sciences) for his interest, support and discussions, particularly in the initial stage of this research study and for his valuable comments on the manuscript. The authors also wish to thank Habil. Dr. Antanas Orliukas and Dr. Algis Kežionis (both of the Department of Radiophysics, Vilnius University, Lithuania) for their interest and discussions concerning problems and results in the field of solid-electrolyte systems based on yttria-stabilized zirconia. The authors also thank Dr. Aloizijs Patmalnieks (Institute of Solid State Physics, University of Latvia) for scanning electron microscopy of our YSZ specimens. XRD data of the powdered specimen were recorded by Çirts Vītiņš in the Department of Chemistry of the Technical University of Denmark

during his scholarship tenure. The authors would like to express their gratitude to the Hewlett-Packard Company and its employee Mr. Markuss Jansons for the donation of the HP 4194 A impedance analyzer.

References

1. Möbius H-H (1997) J Solid State Electrochem 1: 2
2. Chebotin VN, Perfil'ev MV (1978) Electrochemistry of solid electrolytes. Khimiya, Moscow [in Russian]
3. Mogensen M, Bagger C, Aasberg-Petersen K, Christiansen LJ, Sander B, Paulsen JN (1992) An introduction to solid oxide fuel cells. Notat nr. EP92/231. ELSAM's SOFC-Programme, Phase 2. Project Report No. 2. ELSAMPROJEKT A/S, Power Station Engineering, Fredericia, Denmark
4. Ciacchi FT, Crane KM, Badwal SPS (1994) Solid State Ionics 73: 49
5. Kuzjukevics A, Linderoth S, Grabis J (1996) Solid State Ionics 92: 253
6. Kuzjukevics A, Linderoth S (1997) Solid State Ionics 93: 255
7. Grabis J, Steins I, Rasmane D, Heidemane G (1997) J Eur Ceram Soc 17: 1437
8. Bauerle JE (1969) J Phys Chem Solids 30: 2657
9. Verkerk MJ, Middelhuis BJ, Burggraaf AJ (1982) Solid State Ionics 6: 159
10. Bentzen JJ, Andersen NH, Poulsen FW, Sørensen OT, Schram R (1988) Solid State Ionics 28/30: 550
11. Orliukas A, Sasaki K, Bohac P, Gauckler LJ (1991) Ionic conductivity of ZrO_2-Y_2O_3 prepared from ultrafine coprecipitated powders. In: Solid oxide fuel cells. Proc. 2nd Intl Symp, Athens, Greece. Commission of the European Communities – New ways to save energy. Report EUR 13546 EN, pp 377–385
12. Orliukas A, Kezionis A, Paulavicius K, Gauckler LJ, Sasaki K, Bohac P (1994) Solid State Phenom 39–40: 223
13. Gödickemeier M, Michel B, Orliukas A, Bohac P, Sasaki K, Gauckler L, Heinrich H, Schwander P, Kostorz G, Hofmann H, Frei O (1994) J Mater Res 9: 1228
14. Joint Committee on Powder Diffraction Standards (JCPDS). Yttrium zirconium oxide $Y_{0.15}Zr_{0.85}O_{1.93}$. Card No. 30–1468
15. Verkerk MJ, Hammink MWJ, Burggraaf AJ (1983) J Electrochem Soc 130: 70
16. Macdonald JR (ed) (1987) Impedance spectroscopy emphasizing solid materials and systems. Wiley, New York
17. Chebotin VN (1982) Solid state physical chemistry. Khimiya, Moscow, pp 168–189 [in Russian]
18. Sasaki J, Mizusaki J, Yamauchi Sh, Fueki K (1981) Bull Chem Soc Jpn 54: 1688